Available online at www.sciencedirect.com

ScienceDirect

Ceramics International 40 (2014) 4429–4435

CERAMICS INTERNATIONAL

www.elsevier.com/locate/ceramint

Effect of 2-propanol and water contents on the crystallization and particle size of titanium dioxide synthesized at low-temperature

Juha-Pekka Nikkanen*, Elina Huttunen-Saarivirta, Xiaoxue Zhang, Saara Heinonen, Tomi Kanerva, Erkki Levänen, Tapio Mäntylä

Department of Materials Science, Tampere University of Technology, P.O. Box 589, FIN-33101 Tampere, Finland

Received 16 July 2013; received in revised form 27 August 2013; accepted 27 August 2013
Available online 3 September 2013

Abstract

Two series of titanium dioxide, TiO_2, powder were prepared at a temperature of 50 °C without any catalyst. The effects of 2-propanol and water contents on the formation of crystalline powder mixture of anatase and brookite were systematically studied. The characteristics of produced powder were determined by employing X-ray diffraction, transmission electron microscopy, nitrogen adsorption test and Fourier transform infrared spectroscopy.

The obtained results showed that increases in the amount of water used in the powder synthesis turned the product from amorphous to the crystalline anatase structure with small traces of brookite. The results also clearly showed that the use of 2-propanol in the synthesis hindered the crystallization of TiO_2. Furthermore, the specific surface area of TiO_2 nanopowder decreased and the particle size increased when more water was used in the synthesis. These results are presented and discussed in this paper.

Keywords: A. Powders: chemical preparation; A. Sol–gel processes; D. TiO_2

1. Introduction

Titanium dioxide, TiO_2, has three polymorphs: rutile, anatase and brookite. TiO_2 is extensively used in cosmetics, paints and food products because it is stable, inexpensive and non-toxic as well as has a high index of reflection. Photocatalytic activity of TiO_2 has also been widely reported and discussed in literature due to promising applications of TiO_2 in the production of hydrogen or mineralization of several organic pollutants. In photocatalytic applications, the used phases of TiO_2 are anatase and rutile [1–5].

Numerous methods have been employed for the controlled formation of crystalline TiO_2 coatings and nanoparticles. Promising technique is, for example, a sol–gel method, primarily via the hydrothermal and solvothermal processing routes based on alkoxide (M-OR) or titanium(IV) chloride precursors [6–8]. These techniques offer the effective routes to prepare titanium dioxide with a good control of particle size and phase composition as well as high homogeneity in particle distribution [6–9]. In these syntheses methods, precursors are typically dissolved into organic solvent after which they undergo hydrolysis and condensation reactions with the added water. The reactions and the structure of the final product can be controlled by adjusting process parameters, such as temperature and the amount of catalyst [10–12]. The result of hydrolysis and condensation of titanium-containing alkoxide is the formation of (TiO_6) octahedra. The crystal structure of TiO_2 depends on how these octahedra (TiO_6) are linked to each other. Final structure of anatase and rutile is tetragonal, whereas brookite is orthorhombic [12–14]. One method to obtain desired crystal structure of TiO_2 powder is the heat treatment of amorphous titanium hydroxide [15]. However, crystallization by heat treatment has been reported to increase the particle size and to decrease the specific surface area [12–14]. That is the main reason why the low-temperature synthesis methods like hydrothermal, solvothermal and other modified synthesis methods to prepare crystalline TiO_2 are applied [12,13,16–18].

In this study, two series (denoted as S1 and S2) of TiO_2 powders are synthesized by hydrothermal method under

*Corresponding author. Tel. +358 408490193; fax: +358 3 3115 2330.
E-mail address: juha-pekka.nikkanen@tut.fi (J.-P. Nikkanen).

0272-8842/$ - see front matter © 2013 Elsevier Ltd and Techna Group S.r.l. All rights reserved.
http://dx.doi.org/10.1016/j.ceramint.2013.08.115

ambient pressure at a temperature of 50 °C. The first series (S1) was synthesized in a water-alkoxide-2-propanol mixed solution and the another series (S2) in a solution of only water and alkoxide. These two series were synthesized in order to find out the effects of 2-propanol and water contents on the formation of crystalline titanium dioxide at low temperature; to the best of our knowledge, no earlier studies report the influence of the amount of 2-propanol used in the synthesis on the crystallization of TiO_2. The synthesized powders were then characterized in terms of phase composition, specific surface area, particle size, morphology and surface groups involved.

2. Experimental procedure

2.1. Preparation of TiO_2 powders

The starting precursors were tetra-n-butyl orthotitanate alkoxide (denoted as $C_{16}H_{36}O_4Ti$, purity > 98%, VWR), 2-propanol (denoted as C_3H_7OH, purity > 99.5%, VWR) and ion-exchanged water. All chemicals used in this study were reagent-grade and no further purification was done. Two series of powders were synthesized, denoted as S1 and S2. For the powders S1, 1.875 ml tetra-n-butyl orthotitanate liquid was diluted with 6.25 ml of 2-propanol. The solution was stirred for 15 min before a varying amount of ion-exchanged water was added into it. The powders of the first series were labeled as $S1_1$, $S1_2$, $S1_3$, $S1_4$, $S1_5$ and $S1_6$. For the powders S2, a varying amount of ion-exchanged water was added into tetra-n-butyl orthotitanate. 2-propanol was not used at all in the series S2. The obtained powders were labeled as $S2_1$, $S2_2$, $S2_3$, $S2_4$, $S2_5$ and $S2_6$. The molar ratios of water/2-propanol and water/tetra-n-butyl orthotitanate used in the syntheses are listed in Table 1.

After the ion-exchanged water was added into the solutions, these were further stirred for 24 h at 50 °C under atmospheric pressure. After this period, the precipitated powders were separated by filtering and finally dried in a furnace at 50 °C for 24 h. The experimental procedures for processing TiO_2 nanoparticles are described in Fig. 1.

Table 1
The molar ratio of water/2-propanol and water/tetra-n-butyl orthotitanate for powder syntheses.

Sample	The molar ratio of water/2-propanol	The molar ratio of water/tetra-n-butyl orthotitanate
$S1_1$	1.0	15
$S1_2$	1.7	25
$S1_3$	2.3	35
$S1_4$	3.3	50
$S1_5$	7.3	112
$S1_6$	15	230
$S2_1$	–	15
$S2_2$	–	25
$S2_3$	–	35
$S2_4$	–	50
$S2_5$	–	112
$S2_6$	–	230

2.2. Characterization of the powders

The crystal structure of TiO_2 powders was determined by using a Siemens Kristalloflex D-500 X-ray diffractometer and a monochromatized CuKα radiation over the range of $20° < 2\theta < 70°$. The crystal size were estimated from smoothed XRD-patterns, using a Scherrer formula $t = (0.9\lambda / B\cos\theta)$ [19], where t is the size in nm, λ is the wavelength of X-rays in nm (0.15418 nm), B is the full width half maxima of the peak in radians and θ is the Bragg angle. The specific surface area of the powders was measured by nitrogen adsorption tests using a Brunauer–Emmett–Teller (BET) method and Colter Omnisorp 100 cx device. The average size of the particles was calculated using the following equation: $d_{BET} = 6/(\rho S_{ssa})$, where ρ is the density and S_{ssa} is the specific surface area. The morphology of the particles was determined by using a JEOL JEM 2010 transmission electron microscope (TEM) and the accelerating voltage of 200 kV. Surface groups of the powders were examined using a Perkin Elmer Spectrum One Fourier transform infrared spectrometer (FTIR) in the wavenumber range of 4000–450 cm^{-1}.

3. Results

3.1. Structural analysis

Figs. 2 and 3 show the raw XRD patterns for the powder samples. The pattern in Fig. 2(a) shows the amorphous nature of the $S1_1$ precipitate obtained using the lowest water/2-propanol ratio within series S1. The patterns in Fig. 2(b and c) and related to $S1_2$ and $S1_3$ show that the powders were still mainly amorphous, with minor peaks of crystalline anatase phase being also detected. Clear peaks of crystalline anatase phase and a small trace of brookite (121) at $2\theta = 30.8$ were detected in XRD patterns $S1_4$, $S1_5$ and $S1_6$ in Fig. 2(d–f), respectively. The obtained results indicate that after the molar ratio of water/2-propanol was 3.3 only minor changes in the intensity and width of the diffraction peaks occurred (Fig. 2(d–f)) with the increasing amount of water. Hence, the main finding was that the lowest used amount of water yielded an amorphous precipitate but with increases in the amount of water, the precipitate crystallized to anatase with small traces of brookite.

The XRD spectra of powders synthesized without 2-propanol (series S2) are shown in Fig. 3(a–f). The pattern presented in Fig. 3(a) revealed crystalline nature of the powder synthesized with the lowest amount of water ($S2_1$). Although peaks were clearly detectable, the overall intensity of the pattern in Fig. 3(a) was quite low, meaning that the powder $S2_1$ was poorly crystallized. With increase in the amount of water, peaks became more evident and the intensity of the peaks higher, indicating more complete crystallization. However, when comparing the XRD spectra for powders synthesized with 2-propanol (Fig. 2) to those for powders synthesized without it (Fig. 3), it may be clearly seen that the presence of 2-propanol in the precursor solution inhibited the crystallization of TiO_2. With the same amount of water used in the

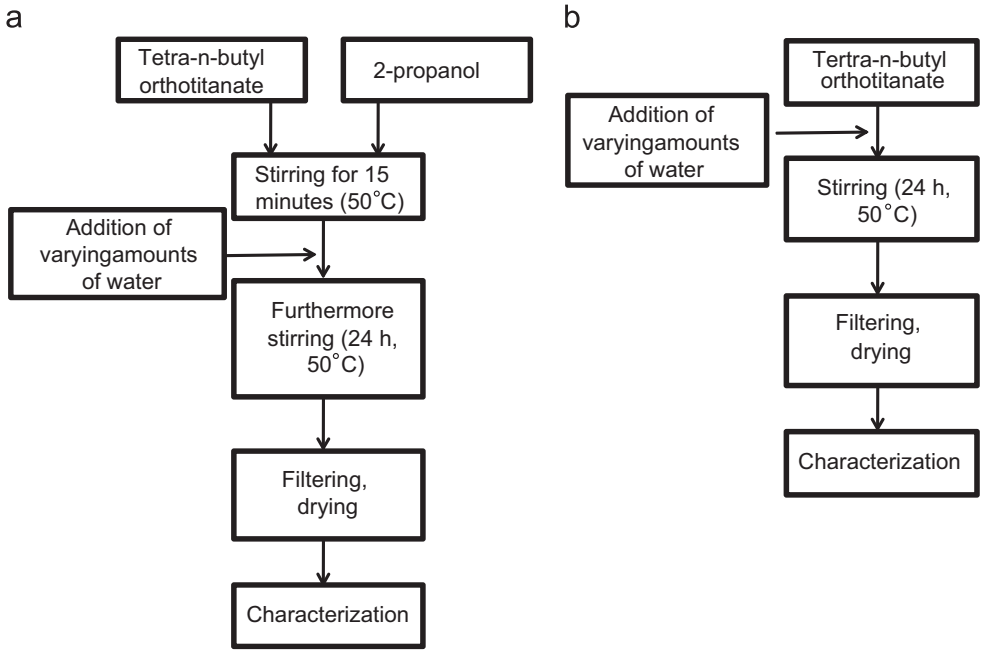

Fig. 1. Flow sheet for the preparation of TiO_2 powders (S1) with 2-propanol (a) and (S2) without 2-propanol (b) in the synthesis.

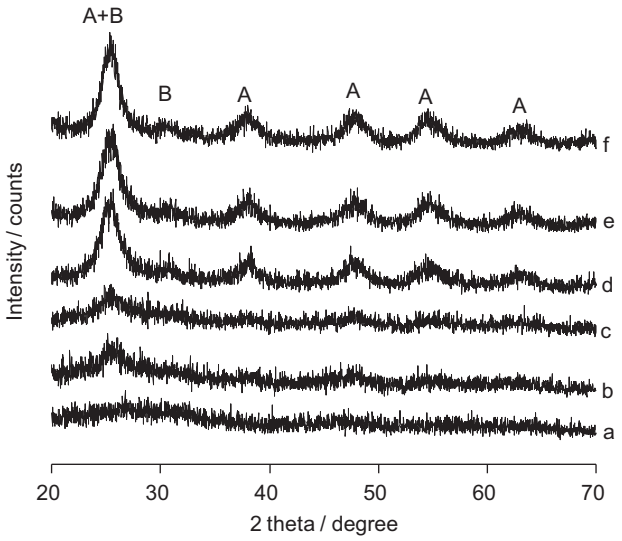

Fig. 2. Raw XRD patterns for synthesized powders with a 2-propanol: (a) $S1_1$, (b) $S1_2$, (c) $S1_3$, (d) $S1_4$, (e) $S1_5$, and (f) $S1_6$; A: anatase and B: Brookite.

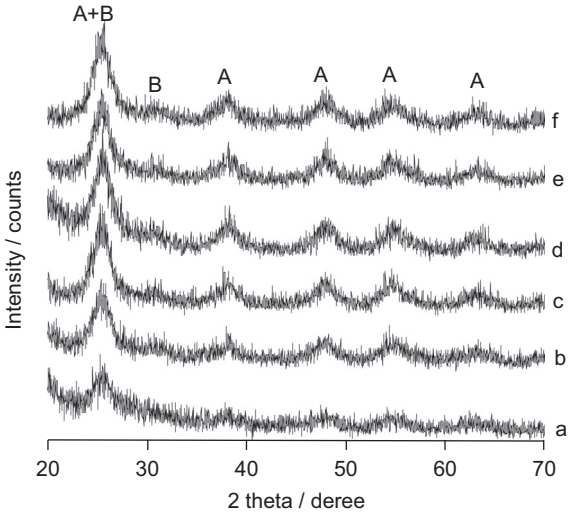

Fig. 3. Raw XRD patterns for synthesized powders without a 2-propanol: (a) $S2_1$, (b) $S2_2$, (c) $S2_3$, (d) $S2_4$, (e) $S2_5$, and (f) $S2_6$; A: anatase and B: Brookite.

syntheses, powder $S1_1$ was amorphous (Fig. 2(a)) but powder $S2_1$ was partially crystallized (Fig. 3(a)). The effect of 2-propanol may also be obtained by comparing the pattern presented in Fig. 2(b) to that in Fig. 3(b) and Fig. 2(c) to that in Fig. 3(c). However, in addition of qualitative evaluation of the crystallization of TiO_2, also quantitative study of the effect of 2-propanol and water contents on the degree of crystallinity of TiO_2 is considered for our future studies.

3.2. Surface area and particle size analyses

In order to find out the effects of 2-propanol and water on the specific surface area and the particle size of the synthesized powders, nitrogen adsorption/desorption measurements were carried out. Fig. 4(a) shows the surface area of the powders S1 synthesized with 2-propanol. The specific surface area was the highest for the powder synthesized with the lowest amount of water ($S1_1$). When the amount of water used in the synthesis increased, the specific surface area of the powders decreased. This decrease was rapid when the amount of water was small but leveled out when the water/2-propanol molar ratio was higher than in $S1_4$, i.e. 3.3. The decrease in the specific surface area refers to a larger particle size or a higher density of the obtained powder particles.

The specific surface area of the powders included in series S2 synthesized without 2-propanol is shown in Fig. 4(b).

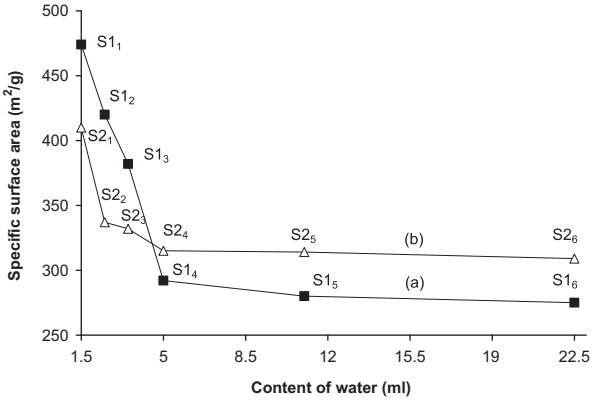

Fig. 4. The effect of the water content on the specific surface area of the samples with 2-propanol (a), and without 2-propanol (b).

Table 2
Specific surface areas and the particle sizes of the samples.

Sample	Crystal size from XRD (nm)	SSA $(g/m)^2$	Particle size from SSSA (nm)
$S1_1$	–	474	(3.2)
$S1_2$	–	420	(3.7)
$S1_3$	–	382	(4.0)
$S1_4$	5.2	292	5.3
$S1_5$	5.3	280	5.5
$S1_6$	5.5	275	5.6
$S2_1$	4.2	410	(3.8)
$S2_2$	4.5	337	(4.6)
$S2_3$	4.6	332	4.6
$S2_4$	4.9	315	4.9
$S2_5$	4.9	314	4.9
$S2_6$	4.9	309	5.0

Again, the specific surface area was the highest for the powder synthesized with the lowest amount of water ($S2_1$). Further increase in the amount of water decreased the specific surface area rapidly to a certain point ($S2_2$). After this point, decrease of the specific surface area slowly leveled out with increase in the amount of added water.

In general, the specific surface area of the powders included in series S1 ($S1_1$, $S1_2$, and $S1_3$) synthesized with 2-propanol were higher than those included in series S2 and synthesized without 2-propanol ($S2_1$, $S2_2$, and $S2_3$). This is probably because the powders synthesized with 2-propanol were clearly less crystallized and, consequently, their density was smaller. However, when comparing the more crystallized powders of $S1_4$, $S1_5$, and $S1_6$ to those of $S2_4$, $S2_5$, and $S2_6$, it can be seen that the specific surface areas were higher when 2-propanol was not used (series S2). This may be explained by the fact that alcohol decreases the dielectric constant of the solvent, leading to decreased stability, enhanced rate of aggregation and, therefore, formation of larger particles [20]. It is probable that the used alcohol also influences the specific surface area of the poorly crystallized powders of series S1 ($S1_1$, $S1_2$, and $S1_3$). However, the main factor influencing the specific surface area of the poorly crystallized powders is evidently the low crystallization and small density of these powders. Still, the potential effect of solvent on the specific surface area needs to be taken into account when aiming at synthesizing non-crystalline solids with a controlled surface area.

Hence here, the specific surface areas of powders ($S1_1$, $S1_2$, and $S1_3$) synthesized with 2-propanol were larger than the specific surface areas of powders synthesized without 2-propanol ($S2_1$, $S2_2$, and $S2_3$), because the powders synthesized with 2-propanol were poorly crystallized. When the amount of added water was adequate to crystallize the powders synthesized with 2-propanol ($S1_4$, $S1_5$, and $S1_6$), the specific surface areas were lower than those of powders synthesized without 2-propanol ($S2_1$, $S2_2$, and $S2_3$) because 2-propanol enhances the formation of larger particles.

The average crystallite size of anatase, estimated from smoothed and background corrected XRD patterns using the Scherrer formula, as well as the average particle size (d_{BET}) are listed in Table 2. It may be seen that the values for the average particle sizes obtained by these two methods are consistent. The particle sizes of $S1_1$, $S1_2$, $S1_3$, $S2_1$ and $S2_2$ are in brackets because the true particle sizes are probably higher than the calculated values. This is due to the amorphous nature of these powders that probably yield densities lower than that of anatase (3.9 g cm^{-3}) [21].

3.3. Morphology of TiO_2 powders

Transmission electron micrographs of the obtained TiO_2 powders $S1_1$, $S1_6$, $S2_1$, and $S2_6$ are shown in Fig. 5(a–d). In all cases, the nanoparticles had the sizes of about 3–7 nm. This is well consistent with the sizes estimated from XRD peaks and the specific surface areas.

3.4. Surface group analysis

IR measurements were performed in order to reveal the effect of the precursor solution water content on the purity of the powders. Fig. 6(a–c) shows the FTIR spectra of the powders $S1_1$, $S1_2$ and $S1_4$. This series is adequate to demonstrate the possible differences in surface groups with different amounts of water. Common factor in the curves ($S1_1$, $S1_2$, and $S1_4$) was the broad peak of Ti–O–Ti at 500 cm^{-1} and the peaks of O–H groups near 1620 and 3400 cm^{-1}. C–H stretching vibrations of alkanes occur in general in the region of 3000–2840 cm^{-1}. More exactly, the absorptions of the $\nu_{as}(CH_3)$, $\nu_{as}(CH_2)$, $\nu_s(CH_3)$ and $\nu_s(CH_2)$ are near 2960, 2926, 2872 and 2853 cm^{-1}, respectively. The positions of these bands do not vary more than ± 10 cm^{-1}in the aliphatic and cyclic hydrocarbons [22]. The positions of these peaks were clearly visible in Fig. 6(a) except for the $\nu_s(CH_3)$ absorption peak, which often overlaps with $\nu_s(CH_2)$ and is therefore difficult to distinguish. In Fig. 6(b) these peaks were weak and in Fig. 6(c) could not be detected at all. The symmetrical bending vibration $\delta_s(CH_3)$ occurs near 1375 cm^{-1} whereas the asymmetrical bending vibration $\delta_{as}(CH_3)$ and symmetrical $\delta_s(CH_2)$ take place near 1450 cm^{-1}[22]. These peaks were

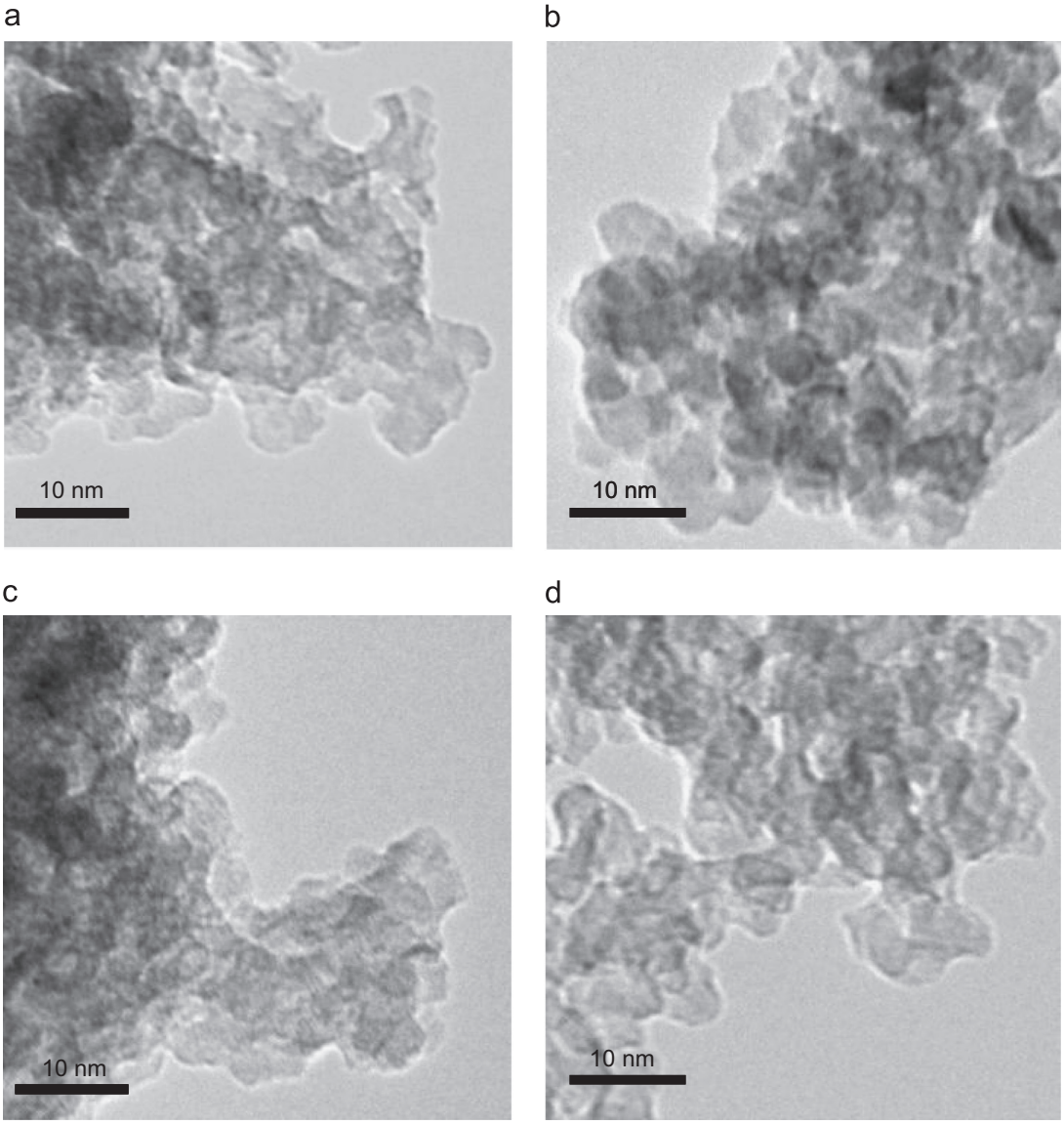

Fig. 5. TEM micrographs of (a) $S1_1$, (b) $S1_6$, (c) $S2_1$, and (d) $S2_6$.

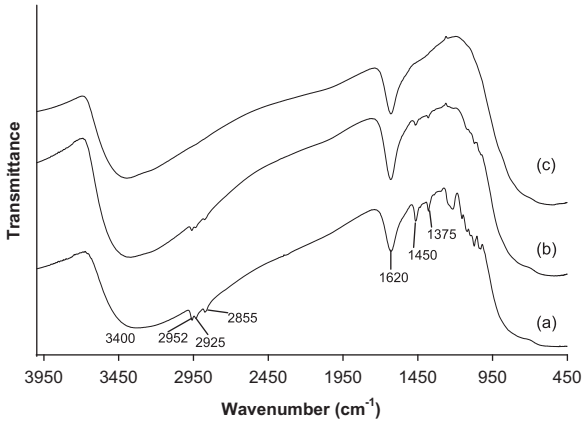

Fig. 6. FTIR spectra of the samples $S1_1$ (a), $S1_2$ (b) and $S1_4$ (c).

also clear in Fig. 6(a), weak in Fig. 6(b) and they did not exist at all in Fig. 6(c). The vibrations between (1350 and 750 cm^{-1}) [22] are too weak to be interpreted by group frequency analysis. However, a comparison of this region (Fig. 6(a)) to the corresponding regions in Fig. 6(b and c) showed clearly that the higher content of water (from $S1_1$ to $S1_4$) in synthesis with 2-propanol enhanced the purity of the surfaces of synthesized titanium dioxide from organic residuals.

Fig. 7(a–c) shows the FTIR spectra of the powders $S2_1$, $S2_2$ and $S2_4$ synthesized without 2-propanol. Common factor in these curves was the broad peak of O–Ti–O and the peaks of O–H groups near 1620 and 3400 cm^{-1}, similarly to Fig. 6. In Fig. 7(a), there were also clear $\nu_{as}(CH_3)$, $\nu_{as}(CH_2)$, $\nu_s(CH_3)$ and $\nu_s(CH_2)$, $\delta_s(CH_3)$, $\delta_{as}(CH_3)$ absorption peaks for the powder

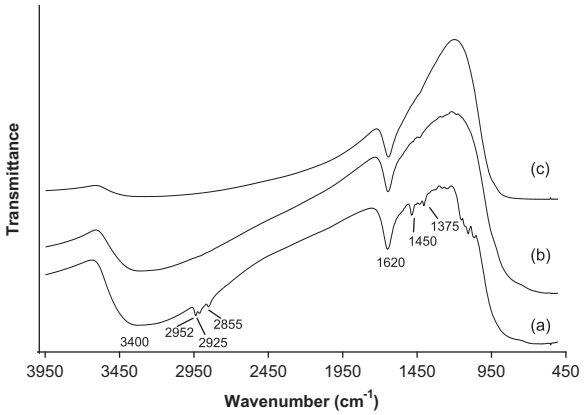

Fig. 7. FTIR spectra of the samples $S2_1$ (a), $S2_2$ (b) and $S2_4$ (c).

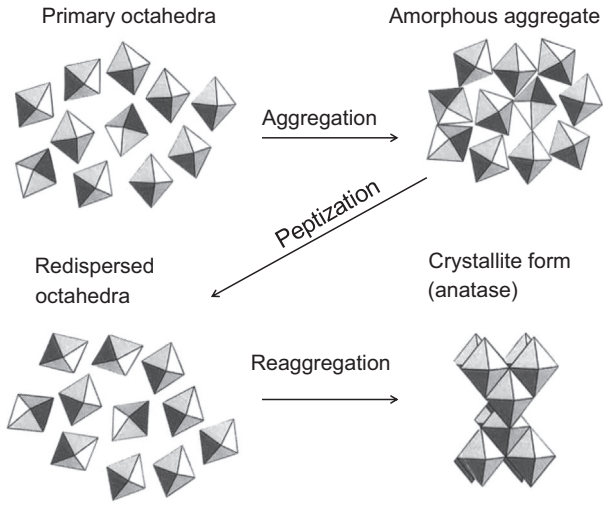

Fig. 8. Proposed mechanism for the formation of anatase in the low temperature synthesis.

$S2_1$. The origin of these peaks is clearly tetra-n-butyl orthotitanate. However, in Fig. 7(b) there were no peaks of $\nu_{as}(CH_3)$, $\nu_{as}(CH_2)$, $\nu_s(CH_3)$ and the peaks of $\nu_s(CH_2)$, $\delta_s(CH_3)$, $\delta_{as}(CH_3)$ were very weak, which means that the slight increases in the amount of water (from $S2_1$ to $S2_2$) in the synthesis without 2-propanol was enough to clean the surfaces of TiO_2 from organic residuals. In Fig. 7(c), there were only absorption peaks of the O–H groups.

When comparing the results from analysis of FTIR spectra (Figs. 6 and 7) to the data obtained from XRD measurements (Figs. 2 and 3) it can be observed that there was a clear connection between the purity and the crystallization of powders. The powder samples which were synthesized with the lowest amount of water contained organic residuals on the surfaces of the amorphous ($S1_1$) and partially crystallized powder ($S2_1$). However, when the used amount of water was higher ($S1_2$, $S2_2$), there were still residuals on the surfaces of the powder synthesized with 2-propanol ($S1_1$) but surfaces of the more crystallized powder synthesized without 2-propanol ($S2_2$) were clean of these residuals. When the amount of water was still increased ($S1_4$, $S2_4$) the surfaces of the samples of both series were completely clean from organic residuals and the formation of anatase structure came possible.

4. Discussion

As the results showed, the presence of 2-propanol in the precursor solution inhibited the crystallization of TiO_2. With the low amount of water used in synthesis, powders prepared with 2-propanol ($S1_1$, $S1_2$, and $S1_3$) were mainly amorphous but powders prepared without 2-propanol ($S2_1$, $S1_2$, and $S1_3$) were more crystallized.

As shortly described in the introduction part, the formation of crystalline TiO_2 nanoparticles straight from a liquid phase is a multiple step-process. After the hydrolysis, condensation and nucleation of (TiO_6) octahedra, these octahedra aggregate and form an amorphous precipitate. In the next step peptization occurs, resulting in the break-up of original bonds within the (TiO_6) octahedra. Finally, the peptisized octahedra undergo slow reaggregation and crystallize so that the overall stoichiometry corresponds to anatase TiO_2 [12,13]. The crystallization pathway of anatase from octahedral is showed in Fig. 8.

Considering the formation of crystalline TiO_2 particles described before, amorphous agglomerates which were formed by fast hydrolysis, condensation and precipitation steps need to break to enable reaggregation of primary particles into the crystalline form. One possible inhibition effect of 2-propanol in the crystallization of TiO_2 observed in our study could be explained by hindered peptization of precipitated agglomerates. According to Vorcapic et al., the formation of TiO_2 colloid is significantly influenced by the used solvent. Alcohols decrease the stability of TiO_2 solution by decreasing the dielectric constant of the solution. The result is enhanced rate of reaggregation and hindered peptization [20]. Similar trends in the presence of alcohols have also been reported for related systems. Park et al. found out in their study that the aggregation of particles in TiO_2 dispersion increases when alcohol is present in the solution [23]. According to their results, the chemical adsorption of residuals from the used alcohol in synthesis lowers the zeta potential of prepared particles. This, together with a low dielectric constant of the solution, promotes the aggregation of the fine precipitates in alcohol-containing solutions. As a result, the peptization process is hindered when alcohols are used [23]. Although neither Vorcapic [20] nor Park [23] investigated the crystallization of TiO_2 in their studies, their findings about the formation of TiO_2 colloids offer valuable information to understand the crystallization behavior of anatase TiO_2 synthesized by a hydrothermal route in a mild environment in our study. Considering the fact that the peptization is needed to break an amorphous structure before the crystallization, it is reasonable to conclude that the hindered peptization together with promoted aggregation through the agency of alcohol hinders not only the peptization but crystallization of TiO_2.

In our study, the hindering effect of alcohol on crystallization of TiO_2 may involve also another mechanism than colloidal destabilization. Yu et al. detected that the existence of alkyl groups in precursors results steric hindrance preventing the phase transition from amorphous to crystalline anatase [24]. As such alkyl groups were detected on the anatase

surfaces, this explanation is viable. As a conclusion, there are two key elements which hinder the crystallization of TiO_2 processed straight from the alkyl containing solution: inhibited peptization of amorphous aggregate and steric hindering caused by alkyl groups adsorbed on the surfaces of primary particles; both of them offer a feasible explanation.

5. Conclusions

In this study, crystalline TiO_2 anatase powder with small traces of brookite has been synthesized at low temperature without any catalyst. The influence of 2-propanol on TiO_2 crystallization was examined for the first time. The crystallization and specific surface area of the synthesized powder were studied as a function of molar ratio of water/2-propanol and water/tetra-n-butyl orthotitanate. It was observed that an increase in the content of water turns the product from amorphous to crystalline and causes the specific surface area to decrease. It was also found that 2-propanol clearly hinders the crystallization of TiO_2. With the lowest amount of water used in the synthesis, the powder synthesized by using 2-propanol was amorphous but powder synthesized without 2-propanol was partially crystallized. It was also observed that the surfaces of the powders synthesized without 2-propanol in synthesis were cleaner from organic residuals than those synthesized with 2-propanol. It is proposed that 2-propanol used in synthesis inhibited the peptization of amorphous precipitate and, due to inhibited peptization, hindered the crystallization of TiO_2. Moreover, it was suggested that the adsorption of alkyl groups on the surfaces of primary particles may cause steric hindering between the particles and prevent the formation of ordered crystalline structure.

Although a more detailed investigation regarding effect of water and solvent contents to the degree of crystallinity of the TiO_2 powders is needed in further studies, the results of this article could be of great importance in both scientific and engineering aspects.

Acknowledgments

The present study is partially supported by The Finnish National Graduate School on New Materials and Processes.

References

[1] A. Fujishima, T.N. Rao, D.A. Tryk, Titanium dioxide photocatalysis, Journal of Photochemistry and Photobiology C: Photochemistry Reviews 1 (2000) 1–21.
[2] A. Fujishima, K. Hashimoto, T. Watanabe, TiO_2 Photocatalysis Fundamentals and Applications, first ed., BKC, Tokyo, 1999.
[3] S. Yang, L. Gao, Preparation of titanium dioxide nanocrystallite with high photocatalytic activity, Journal of the American Ceramic Society 88 (2005) 968–970.
[4] A. Houas, H. Lachleb, M. Ksibi, E. Elalui, C. Guillard, J.-M. Herrmann, Photocatalytic degradation pathway of methylene blue in water, Applied Catalysis B: Environmental 31 (2001) 145–157.
[5] T. Minabe, D.A. Tryk, P. Sawunyama, Y. Kikuchi, K. Hashimoto, A. Fujishima, TiO_2-mediated photodegradation of liquid and solid organic compounds, Journal of Photochemistry and Photobiology A: Chemistry 137 (2000) 53–62.
[6] C.J. Brinker, G.W. Scherer, Sol–gel Science: the Physics and Chemistry of Sol–gel Processing, Academic Press, Inc., 1990.
[7] G. Li, K.A. Gray, Preparation of mixed-phase titanium dioxide nanocomposites via solvothermal processing, Chemistry of Materials 19 (2007) 1143–1146.
[8] G. Li, S. Ciston, Z.V. Saponjic, L. Chen, N.M. Dimitrijevic, T. Rajh, K.A. Gray, Synthesizing mixed-phase TiO_2 nanocomposites using a hydrothermal method for photo-oxidation and photoreduction applications, Journal of Catalysis 253 (2008) 105–110.
[9] K.-N. Kumar, K. Keizer, A. Burggraaf, T. Okubo, H. Nagamoto, S. Marooka, Densification of nanostructured titania assisted by a phase transformation, Nature 358 (1992) 48–51.
[10] K.-N. Kumar, H. Izutsu, D.-J. F, Y. Chabal, T. Okubo, Alcohol washing as a way to stabilize the anatase phase of nanostructured titania through controlling particle packing, Journal of Materials Science 44 (2009) 5944–5948.
[11] H.-F. Yu, S.-M. Wang, Effects of water content and pH on gel-derived TiO_2–SiO_2, Journal of Non-crystalline Solids 261 (2000) 260–267.
[12] M. Gobal, W.J. Moberly Chan, L.C. De Jonghe, Room temperature synthesis of crystalline metal oxides, Journal of Materials Science 32 (1997) 6001–6008.
[13] S. Watson, D. Beydoun, J. Scott, R. Amal, Preparation of nanosized crystalline TiO_2 particles at low temperature for photocatalysis, Journal of Nanoparticle Research 6 (2004) 193–207.
[14] K. Ding, Z. Miao, B. Hu, G. An, Z. Sun, B. Han, Z. Liu, Study on the anatase to rutile nanocrystals with the assistance of ionic liquid, Langmuir 26 (2010) 10294–10302.
[15] J.S. Reed, Introduction to the Principles of Ceramic Processing, John Wiley, New York41.
[16] J.-P. Nikkanen, E. Huttunen-Saarivirta, T. Kanerva, V. Pore, T. Kivelä, E. Levänen, T. Mäntylä, Photoactive TiO_2 nanopowder synthesized at low temperature without a catalyst, Journal of Ceramic Science and Technology 02 (2011) 97–102.
[17] C.-C. Wang, J.Y. Ying, Sol–gel synthesis and hydrothermal processing of anatase and rutile titania nanocrystals, Chemistry of Materials 11 (1999) 3113–3120.
[18] J.-P. Nikkanen, T. Kanerva, T. Mäntylä, The effect of acidity in low-temperature synthesis of titanium dioxide, Journal of Crystal Growth 304 (2007) 179–183.
[19] B.D. Cullity, Elements of X-ray Diffraction, Addison-Wesley Publishing Company Inc., USA, 1967.
[20] D. Vorkapic, T. Matsoukas, Effect of temperature and alcohols in the preparation of titania nanoparticles from alkoxides, Journal of the American Ceramic Society 81 (1998) 2815–2820.
[21] Handbook of Chemistry and Physics, CRC Press, Inc., 55th edition, USA, 1974.
[22] R.M. Silverstein, F.X. Webster, Spectrometric Identification of Organic Compounds, 6th edition, John Wiley & Sons, Inc., Canada, 1996.
[23] H.K. Park, D.K. Kim, C.H. Kim, Effect of solvent on titania particle formation and morphology in thermal hydrolysis of $TiCl_4$, Journal of the American Ceramic Society 80 (1997) 743–749.
[24] J. Yu, G. Wang, B. Cheng, M. Zhou, Effects of hydrothermal temperature and time on the photocatalytic activity and microstructures of bimodal mesoporous TiO_2 powders, Applied Catalysis B 69 (2007) 171–180.